

Effect of boron and aluminum diboride on ignition of high-energy materials

Alexander G. Korotkikh^{*,***†}, Ivan V. Sorokin^{*},
Ekaterina A. Selikhova^{*}, and Vladimir A. Arkhipov^{**}

^{*}Tomsk Polytechnic University, 634050, 30 Lenin Pros., Tomsk, RUSSIA

Phone: +7-382-270-1777

[†] Corresponding author: korotkikh@tpu.ru

^{**}Tomsk State University, 634050, 36 Lenin Pros., Tomsk, RUSSIA

Received: April 26, 2018 Accepted: January 30, 2019

4
2
9

Abstract

The high heat of oxidation makes boron and diborides attractive as a metal fuel additive in high-energy materials (HEM) and solid propellants. This study investigates the laser ignition for the HEM samples based on ammonium perchlorate, ammonium nitrate, energetic binder and boron-containing components. Micron-sized powders of aluminum, amorphous boron and aluminum diboride were used as the metal fuels in composition of the AP/AN/PMVT/Me HEM samples. We defined the ignition delay time, the surface temperature of the reaction layer during the heating and ignition, the kinetic parameters for the aluminum-based and boron-based HEM samples. It was found that the use of amorphous boron in the HEM sample leads to a decrease in the ignition delay time of the sample by a factor of 2.2–2.8 due to high chemical activity and a difference in the oxidation mechanism of boron particles. The use of aluminum diboride powder in the HEM sample makes it possible to reduce the ignition delay time by 1.7–2.2 times at the same heat flux density in comparison with the aluminum-based HEM sample. It was also shown that the use of boron components leads to an increase in the maximum surface temperature at the time of the flame appearance and to a decrease in the activation energy of ignition.

Keywords: high-energy material, amorphous boron, aluminum diboride, ignition delay time, ignition temperature

1. Introduction

Boron and its compounds are among the most promising metal fuel components to be used in solid propellants for solid fuel rocket motor and ramjet engine. The specific energy released during boron oxidation is one of the highest values per unit mass or volume¹⁾. However, its application is significantly complicated by the fact that the inert B_2O_3 layer is formed on the boron particle surface during storage and combustion. This layer prevents the access of oxidizer²⁾ and increases the ignition delay time and burning time for particles^{3), 4)}.

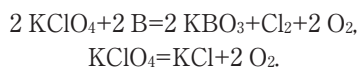
Papers studying boron oxidation mostly focus on two areas: oxidation of single particles^{5), 6)} and powders^{7)–10)} of boron, as well as the boron-based composite solid propellants^{11), 12)}. The increase in the particle size leads to an increase in the thickness of the oxide layer²⁾ and the

ignition temperature, which also has a negative effect on the combustion parameters¹⁰⁾. The combustion mechanism is changed at higher temperatures (~ 2200 °C¹³⁾). The boron oxide layer evaporates and burns in the gas phase. To improve the combustion parameters, additives of metal powders and their oxides are used: magnesium, aluminum, bismuth, cerium, iron, copper^{6), 7)}. This reduces the ignition delay time for additives by up to 2 times⁶⁾ and the ignition temperature by up to 10% (685 °C). The introduction of such additives can also increase the completeness of the conversion^{6)–8)}, which makes the use of bimetal powders one of the most promising areas of study.

Numerous research findings have been published on the ignition and combustion characteristics for boron-containing high-energy materials (HEM) with different

dispersity of metallic fuel¹⁴⁾, oxidizer (most commonly used are NH₄ClO₄, KNO₃) and combustible-binder, and the equivalence ratio of ox-red elements for HEM composition^{13),15)}. A continuous CO₂ laser is used to initiate combustion of HEM in studies of the spectral characteristics and representative temperatures of the flame at atmospheric pressure^{2),15)}. Studies focusing on combustion under high pressures¹⁶⁾ or near-real conditions^{1),13),17)} use the conductive initiation (for example, heating with a nichrome filament¹⁶⁾ or heated gases of a thermal analyzer chamber^{6),7)}). It was established that with an increase in the pressure and the boron content to 20 wt.% in the HEM composition, the burning rate and the surface temperature of the sample are increased, with the pressure dependence close to linear¹¹⁾.

Compared to the combustion of single boron particles, the pressure exponent of the burning rate is higher, due to an increase in the thermodynamically equilibrium fraction of the condensed combustion products in reaction products, which reduces two-phase losses¹⁾. In view of the much greater variety of substances and elements in such systems (compared to the combustion of single metal particles), the reaction mechanism in them is much more complicated and much less studied. The main reaction in the combustion of metals with a solid oxidizer in the form of perchlorate is the oxidation of boron and the decomposition of perchlorate¹⁸⁾:



Various techniques have been used to improve the characteristics of boron-based HEM. The most promising are the use of coatings¹⁹⁾ increasing the particle reactivity and the use of bimetallic powders^{12),20)} with the ignition.

In this study, we investigated the HEM samples based on micron powders of aluminium, amorphous boron and aluminum diboride to determine the ignitability, ignition delay time as a function of the heat flux density, and the corresponding surface temperature of HEM.

2. Experimental methods

2.1 Materials

We used three HEM samples to determine the ignition characteristics. The first HEM sample (marked as μAl) contained 15 wt.% ammonium perchlorate (fraction with particle size of 160–315 μm), 35 wt.% ammonium nitrate (fraction < 100 μm), 20 wt.% energetic binder (PMVT poly methyl-vinyl tetrazole) and 30 wt.% aluminum powder (the mean diameter $d_{43} = 10.8 \mu\text{m}$). In the other samples, aluminum powder was substituted by amorphous boron powder ($d_{43} = 2.0 \mu\text{m}$), aluminum diboride powder ($d_{43} = 6.2 \mu\text{m}$) obtained by the SHS method and contained 55.5 wt.% Al and 44.5 wt.% B (Table 1).

2.2 Ignition method

The ignition process was studied via the setup for radiant heating based on a CO₂ laser with 10.6 μm wavelength and 200 W power (Figure 1). The laser beam

Table 1 The tested HEM samples.

HEM sample	Content [wt.%]			
	AP	AN	PMVT	Me powder
Sample 1	15	35	20	30, μAl
Sample 2	18	42	25	15, B
Sample 3	15.6	36.4	23	25, AlB ₂

The equivalence ratio of the tested HEM samples is 0.6.

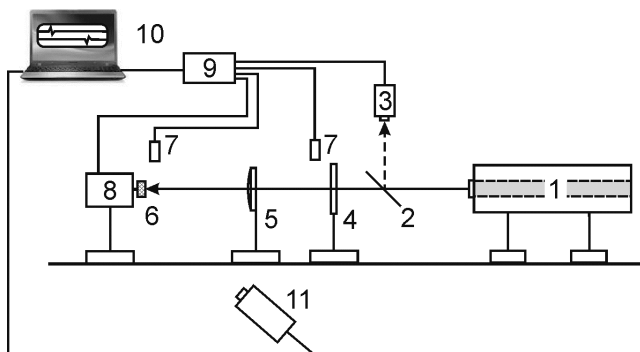


Figure 1 The scheme of experimental setup based on CO₂ laser: 1 - CO₂ laser; 2 - beam-splitting mirror; 3 - thermal power sensor; 4 - shutter; 5 - lens; 6 - HEM sample; 7 - photodiodes; 8 - holder; 9 - ADC; 10 - PC; 11 - thermal imager.

diameter at the exit from the translucent mirror of the CO₂ laser was approximately equal to the diameter of the HEM sample. The HEM samples were cut into 5 mm high tablets before the experiment. The flat end surface of the sample was visually monitored for the absence of pores, depressions and cracks.

The test HEM sample (6) was attached to the holder (8). When the shutter (4) was opened, the heat flux was directed to the HEM sample. The signals from the photodiodes (7) were transmitted through an analog-to-digital converter (9) (ADC, model E-14-440 manufactured by L-CARD Co.) and recorded using a personal computer (10); afterwards, they were processed using the special software (LGraph2, L-CARD Co.). The ignition delay time t_{ign} of the HEM sample was defined as a time difference between the signals from the photodiodes (7), one of which registered the occurrence of flame on the flat end surface of the sample, and the other recorded the opening of the shutter (4). The relative error for the ignition delay time values was equal to 5–12 % at the 0.95 confidence level.

The surface temperature of the HEM sample during the heating and ignition was recorded using a thermal imaging camera (Jade J530 SB) at a frame frequency of 50 Hz and the temperature range of 370–1800 °C. The thermal imaging data and the photodiode parameters were synchronized by a characteristic click produced by shutter opening, which corresponded to the heating start of the HEM sample.

The average and maximum powers of the laser radiation on the HEM surface were measured using a thermal power sensor (3) (Ophir FL400A-BB-50). To determine a maximum power in the center of the laser beam, we used a diaphragm with 2 mm diameter. The ratio between the maximum and mean thermal power

over the area was ~1.7.

2.3 Activation energy

The activation energy was determined by solving the inverse heat conduction problem when heating the sample by a radiative flux following the method in [21]. This method is based on the equation:

$$\ln\left(\frac{t_{ign}}{(1-T_0/T_{ign})^2}\right) = \ln\left(\frac{0.35 \cdot E \cdot c}{(1-0.8 \cdot \beta) \cdot R \cdot Qz}\right) + \frac{1}{\beta}$$

where t_{ign} is the ignition delay time, s; T_0 the initial temperature of the HEM sample, K; T_{ign} the quasi-steady ignition temperature of the HEM sample, K; E the effective activation energy of the reaction, J mol⁻¹; c the specific heat of the HEM sample, J(kg K)⁻¹; $\beta = R \cdot T_{ign}/E$ the unit-less parameter expressing the degree of the dependence of the reaction rate on temperature; R the universal gas constant, J(mole K)⁻¹; Q the specific (per unit weight) heat of the reaction, J kg⁻¹; z the pre-exponential factor, 1 s⁻¹.

The value of the quasi-steady ignition temperature can be determined by the following formula:

$$T_{ign} = T_0 + 1.2q \sqrt{\frac{t_{ign}}{\lambda \cdot c \cdot \rho}}$$

where q is the radiative heat flux density, W cm⁻²; λ, ρ are the thermal conductivity and the density of the HEM sample, W (m·K)⁻¹ and kg m⁻³.

3. Results and discussion

3.1 Ignition delay time

Figure 2 shows the dependences of the ignition delay time for the HEM samples on the mean radiative heat flux density.

The experimental dependences obtained were fitted to a power function of the following form:

$$t_{ign} = A \cdot q^{-B}$$

where t_{ign} is the ignition delay time of the HEM sample, s; q the heat flux density, W m⁻², A, B are fitted constants.

Fitted constants and determination coefficient R^2 for the experimental data are given in Table 2.

A replacement of aluminum with amorphous boron powder results in a decrease in the ignition delay time of the HEM sample by 2.2–2.8 times in the range of heat flux density of 90–200 W cm⁻². The use of aluminum diboride powder makes it possible to reduce the ignition delay time of the HEM sample by 1.7–2.2 times in comparison with the Al-based composition. The difference of the ignition delay time for the HEM samples heated by a radiant flux depends on the oxidation rate and the heat released from the chemical reaction for the metal fuels under study. The Al-based HEM sample is characterized by the long heating and ignition times of the thermal layer. This sample contains coarse aluminum particles covered by a refractory Al₂O₃ oxide layer. The oxide layer increases the heating time of the particles and the HEM sample and prevents the reaction of oxygen with aluminum. When the aluminum melts and expands, the oxide layer on the

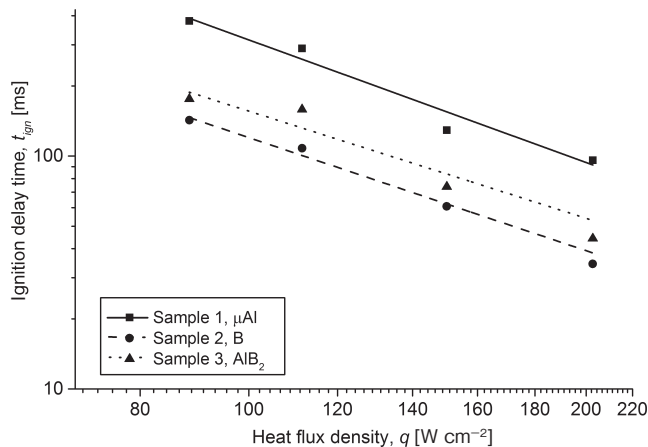


Figure 2 The ignition delay time of the HEM samples vs. the heat flux density.

Table 2 Fitted constants and determination coefficient for the experimental data.

HEM sample	$A, 10^5$	B	R^2
μAl	989.9	1.75	0.96
B	202.3	1.61	0.98
AlB ₂	177.5	1.53	0.87

particle surfaces breaks and an exothermic reaction occurs. When boron or aluminum diboride particles containing 44.5 wt.% of boron are heated, the B₂O₃ oxide layer on the particle surface melts (at a temperature of 450 °C) and gasifies. Accordingly, the reaction of oxygen with boron or boron/aluminum occurs more intensively near the reaction layer surface of the HEM sample, which leads to an increase in heat release and a decrease in the heating time as well as the ignition delay of the HEM sample. Ignition of boron and aluminum diboride particles occurs faster and at lower temperatures.

3.2 Ignition temperature

Synchronized frames of video and thermal imaging are obtained corresponding to the main stages of the ignition for the tested HEM samples. Figure 3 shows the maximum and mean temperatures on the surface of the HEM sample as a function of the heating time and the frames of thermal imaging by Jade J530 SB for the HEM samples at the time of the flame appearance and steady ignition at $q = 115$ W cm⁻². The surface temperatures on the reaction layer for the HEM samples were measured (Table 3) at a constant emissivity of 0.9, which was determined at the use of a spherical photometer.

The process of heating and ignition for the tested HEM samples can be divided into two stages characterized by the formation time and thickness of the heated layer and the rate of temperature rise on the surface of the sample reaction layer due to the oxidation of metal particles. The time period of heating and formation of the reaction layer is the longest for the Al-based HEM sample accompanied by a slow increase in the surface temperature. That is probably due to the aluminum melting in the heated layer. The use of boron and aluminum diboride powders accelerates the exothermic reaction of oxidation with

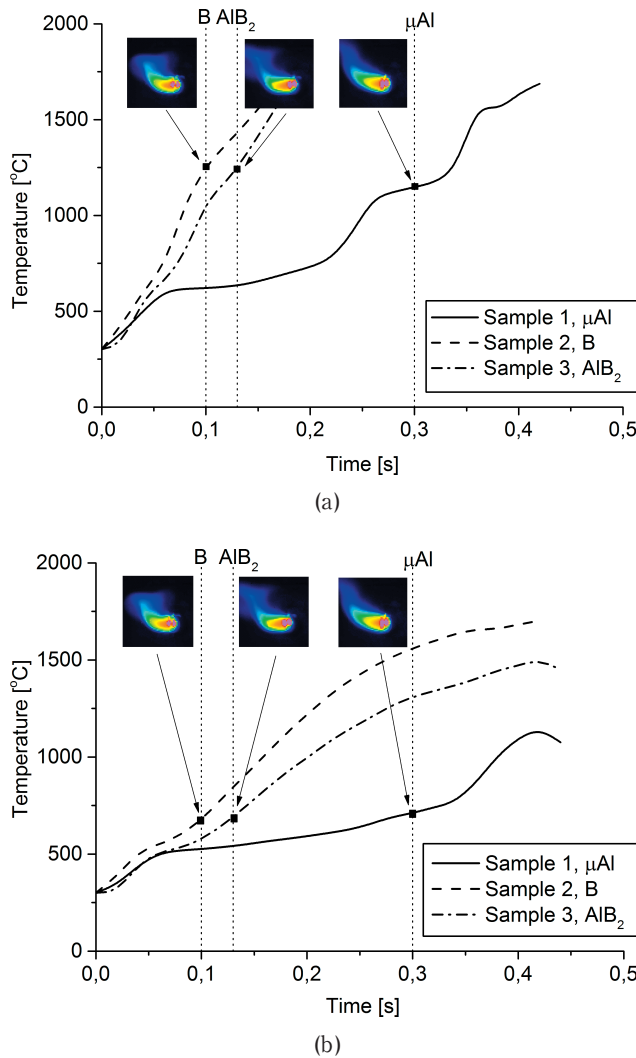


Figure 3 The maximum (a) and mean (b) surface temperatures of the HEM samples vs. the heating time (the points correspond to the ignition time).

Table 3 Surface temperatures for the HEM samples at the time of steady ignition ($q = 115 \text{ W cm}^{-2}$).

HEM sample	Temperature [°C]	
	Maximum	Mean
μAl	1150	710
B	1260	680
AlB ₂	1240	690

additional heat release in the heated layer and near the burning surface at the ignition of the HEM samples and, as a result, increases the maximum surface and initial decomposition temperatures of the oxidizer, an energetic binder and the oxidation of metal particles.

The maximum and mean surface temperatures for the HEM samples containing B and AlB₂ powders are fairly close, which may be due to the same oxidation mechanism of boron-based particles during the radiant heating and ignition of the HEM composition.

3.3 Activation energy

The activation energy, the pre-exponential factor and the quasi-steady ignition temperature for the HEM

Table 4 Calculation data of the formal kinetic parameters for the HEM samples.

HEM sample	$E \text{ [kJ mol}^{-1}\text{]}$	$Qz \text{ [W g}^{-1}\text{]}$	$T_{ign} \text{ [K] at } q = 115 \text{ [W cm}^{-2}\text{]}$
μAl	158.9	9.92×10^{13}	846
B	90.2	3.31×10^{11}	641
AlB ₂	73.6	4.24×10^9	687

samples were determined. Calculation results are shown in Table 4. The Al-based HEM sample has the highest activation energy and quasi-steady temperature of ignition, while those of AlB₂-based HEM sample are the lowest. Based on these data and ignition experimental results, it can be concluded that the use of AlB₂ powder in the HEM composition is preferred in terms of its ignitability.

4. Conclusion

The experimental study of the ignition for the HEM based on ammonium perchlorate, ammonium nitrate and energetic combustible binder determined the ignition delay time, the surface temperature of the reaction layer, the ignition temperature and the activation energy. It was found that the ignition delay time for the HEM sample containing amorphous boron decreases by a factor of 2.2–2.8 in comparison with the HEM sample containing aluminum ASD-4 in the range of the heat flux density of $q = 90\text{--}200 \text{ W cm}^{-2}$ due to acceleration of the exothermic reactions at the increase of temperature for the decomposition of oxidizers and an energetic binder and at the oxidation of boron.

The use of aluminum diboride in the HEM sample makes it possible to reduce the ignition delay time by 1.7–2.2 times in the said range of q as compared to the HEM sample containing aluminum powder. This results from the increased efficiency and heat of oxidation for boron with aluminum in the zone of chemical reactions at the same time, the maximum surface temperature of the HEM sample at the ignition moment increases by 8% and the activation energy decreases by a factor of 2.1.

The reported study was supported by the Tomsk State University and the Tomsk Polytechnic University competitiveness improvement programmes.

Acknowledgment

The reported study was supported by the Tomsk State University and the Tomsk Polytechnic University competitiveness improvement programs, and by RFBR, project number 19-33-90015.

References

- 1) A. Gany and Y.M. Timnat, *Acta Astronautica*, 29, 181–187 (1993).
- 2) W. Ao, J.H. Zhou, J.Z. Liu, W.J. Yang, Y. Wang, and H.P. Li, *Combust., Explos. Shock Waves*, 50, 262–271 (2014).
- 3) K.-L. Chintersingh, M. Schoenitz, and E.L. Dreizin, *Combust. Flame*, 173, 288–295 (2016).
- 4) G. Young, K. Sullivan, M.R. Zachariah, and K. Yu, *Combust.*

- Flame, 156, 322–333 (2009).
- 5) R.O. Foelsche, R.I. Burton, and H. Krier, Combust. Flame, 117, 32–58 (1999).
- 6) J. Xi, J. Liu, Y. Wang, Y. Hu, Y. Zhang, and J. Zhou, Journal of Propulsion and Power, 30, 47–53 (2014).
- 7) J-Z. Liu, J-F. Xi, W-J. Yang, Y-R. Hu, Y-W. Zhang, Y. Wang, and J-H. Zhou, Acta Astronautica, 96, 89–96 (2014).
- 8) L-J. Liu, G-Q. He, and Y-H. Wang, J. Therm. Anal. Calorim., 114 1057–1068 (2012).
- 9) W. Ao, J.H. Zhou, W.J. Yang, J.Z. Liu, Y.J. Wang, and K.F. Cen, Combust. Explos. Shock Waves, 50, 664–669 (2014).
- 10) A. Jain, S. Anthonysamy, K. Ananthasivan, and G.S. Gupta, Thermochim. Acta, 500, 63–68 (2010).
- 11) T. Kuwahara and N. Kubota, Propellants, Explos., Pyrotech., 14, 43–46 (1989).
- 12) A.G. Korotkikh, V.A. Arkhipov, O.G. Glotov, V.E. Zarko, and A.B. Kiskin, Combust. Flame, 178, 195–204 (2017).
- 13) A. Ulas, K.K. Kuo, and C. Gotzmer, Combust. Flame, 127, 1935–1957 (2001).
- 14) F. Maggi, A. Bandera, L. Galfetti, L.T. De Luca, and T.L. Jackson, Acta Astronautica, 66, 1563–1573 (2010).
- 15) D. Liang, J. Liu, J. Zhou, Y. Wang, and Y. Yang, J. Energ. Mater., 34, 297–317 (2016).
- 16) L. Galfetti, L.T. De Luca, F. Severini, L. Meda, G. Marra, M. Marchetti, M. Regi, and S. Bellucci, J. Phys.: Condens. Matter, 18, 1991–2005 (2006).
- 17) T.L. Connell Jr., G.A. Risha, R.A. Yetter, C.W. Roberts, and G. Young, Journal of Propulsion and Power, 31, 373–385 (2014).
- 18) P-J. Liu, L-L. Liu, and G-Q. He, J. Therm. Anal. Calorim., 124, 1587–1593 (2016).
- 19) J.F. Xi, J.Z. Liu, Y. Wang, H.P. Li, Y.W. Zhang, J.H. Zhou, and K.F. Cen, Journal of Solid Rocket Technology, 36, 654–659 (2013).
- 20) A. Abraham, H. Nie, M. Schoenitz, A.B. Vorozhtsov, M. Lerner, A. Pervikov, N. Rodkevich, and E.L. Dreizin, Combust. Flame, 173, 179–186 (2016).
- 21) V. N. Vilyunov and V. E. Zarko, “Ignition of Solids”, Elsevier (1989).